Phase transitions in the urea/n-nonadecane system by calorimetric techniques

2007 J. Phys.: Condens. Matter 19 186221

(http://iopscience.iop.org/0953-8984/19/18/186221)

IOP PUBLISHING JOURNAL OF PHYSICS: CONDENSED MATTER

J. Phys.: Condens. Matter **19** (2007) 186221 (16pp) doi:10.1088/0953-8984/19/18/186221

Phase transitions in the urea/n-nonadecane system by calorimetric techniques

A López-Echarri[1], I Ruiz-Larrea[2], A Fraile-Rodríguez[3], J Díaz-Hernández[4], T Breczewski[2] and E H Bocanegra[2]

[1] Departamento de Física de la Materia Condensada, Facultad de Ciencia y Tecnología, Universidad del País Vasco, Apartado 644, 48080 Bilbao, Spain
[2] Departamento de Física Aplicada II, Facultad de Ciencia y Tecnología, Universidad del País Vasco, Apartado 644, 48080 Bilbao, Spain
[3] Swiss Light Source, Paul Scherrer Institut, 5232 Villigen PSI, Switzerland
[4] Facultad de Ciencias Físico-Matemáticas, Universidad Autónoma de Puebla, Mexico

E-mail: a.lopezecharri@ehu.es

Received 7 November 2006, in final form 19 March 2007
Published 11 April 2007
Online at stacks.iop.org/JPhysCM/19/186221

Abstract

A calorimetric study of urea/n-nonadecane, $CO(NH_2)_2/C_{19}H_{40}$, and the deuterated derivatives, $CO(ND_2)_2/C_{19}D_{40}$ and $CO(NH_2)_2/C_{19}D_{40}$, around the structural phase transition temperature is presented. For this purpose differential scanning (DSC), temperature-modulated (AC) and adiabatic calorimetry have been used and the obtained results are compared. Leaving apart the noticeable peak associated with the main phase transition at 158.5, 149.4 and 154 K respectively, small anomalies of the specific heat are found at lower temperatures and their corresponding entropic and enthalpic changes are reported. Heating and cooling experiments show the influence of the temperature rate and the thermal history on the detailed profile of the specific heat traces. The presence of thermal hysteresis and latent heat as a way to characterize the order of the phase transitions is discussed. Finally, a tentative approach to the urea and the alkyl chain contributions to the specific heat and their influence on the phase transition mechanisms is presented.

1. Introduction

Urea/n-nonadecane, $CO(NH_2)_2/C_{19}H_{40}$, fully deuterated urea/n-nonadecane, $CO(ND_2)_2/C_{19}D_{40}$, and partially deuterated urea/n-nonadecane, $CO(NH_2)_2/C_{19}D_{40}$ (in the following C19, d-C19, and pd-C19 respectively), belong to the so called alkane–urea inclusion compounds. At room temperature they are characterized by linear hexagonal tunnels of ∼0.55 nm diameter formed by helical ribbons of urea molecules (host substructure) where long chain alkanes (guest molecules) are accommodated inside them [1–3]. Each helical pitch (1.102 nm) contains six urea molecules, whereas the nonadecane length is 2.636 nm, which leads to an incommensurate lattice along the hexagonal axis. At low temperatures, most of these compounds present a phase

transition characterized by the distortion of the urea lattice from hexagonal to orthorhombic symmetry, which permits the reorientation of the alkane molecules. The ordering of these molecules in the low temperature phase and their dynamic properties have been studied in detail by means of various experimental techniques such as x-ray diffraction [4, 5], infrared and Raman scattering [6–8], H and D nuclear magnetic resonance (NMR) [9–14], incoherent quasi-elastic neutron scattering [15, 16], neutron scattering under hydrostatic pressure [17], light scattering and Brillouin spectroscopy [18, 19], specific heat measurements [20–22], and molecular mechanism calculations [23–27]. While the ordering process can be related to an indirect coupling with a transverse acoustic phonon of the urea host lattice [28], the detailed mechanisms are yet to be understood and the order character assigned to these phase transitions is still under discussion. Urea/n-heptadecane (in the following C17) shows a neat first order character, as suggested from birefringence measurements and confirmed by calorimetric results [29] and phase boundary studies. However, the experiments carried out on C19, which only differs in two CH_2-groups in the alkyl chain, do not permit a definitive assignment. In this case, phase boundaries are not observed and birefringence results are not conclusive [30]. This fact together with the anomalous specific heat behaviour around the phase transition of the C17 compound, which showed a noticeable dependence on the thermal history and on the measurement temperature rates, has motivated the present study. For this purpose, various calorimetric techniques such as differential scanning (DSC), temperature-modulated (AC), and adiabatic calorimetries were employed on C19 and its deuterated derivatives d-C19 and pd-C19. The combination of these techniques tries to attain a reliable description of the intrinsic thermal properties around the phase transition, where very subtle effects are observed. This methodology may exclude spurious effects due to the sample physical state (powder or single crystal) and can avoid the particular shortcomings of the various experimental techniques.

2. Experimental techniques

Single crystals of C19 were grown by using the isothermal dynamic method at 313 K by slow evaporation of a saturated solution of chemically pure urea and nonadecane compounds in a 50% propanol–methanol mixture. The deuterated crystals were synthesized in a similar way. The single crystals were colourless, transparent, and hexagonal prismatic along the *c*-crystallographic axes. Powdered samples obtained from these crystals were used for DSC and adiabatic calorimetry measurements. On the other hand, single crystals for AC calorimetry experiments were selected. Chemical analysis together with x-ray powder diffraction and precession photographs confirmed the good chemical and structural quality of the samples obtained.

DSC measurements from 170 to 300 K with 1–12 K min^{-1} heating and cooling rates were performed in Perkin-Elmer DSC-7 commercial equipment. Depending on the heating rate, the specific heat accuracy is limited to 2–10%.

AC calorimetry measurements were made by using the experimental installation described in [31]. The basis of this technique lies in the application of a modulated heat source as the way to obtain the specific heat. In our case, a chopped light heats the sample periodically around its mean temperature T_s. The sample is thermally anchored to a heat reservoir (a copper thermal block) at temperature $T_b = T_s \pm \Delta T_{DC}$. The theory was first developed by Sullivan and Seidel [32] by using the thermal conduction equations and the energy conservation law. The measurements permit us to obtain both the amplitude and phase of the temperature oscillation for a slab-shaped sample. The general solution for the sample thermal oscillations (ΔT_{AC}) is

$$\Delta T_{AC} = \frac{P_0}{\omega C_p}\left[1 + \frac{1}{\omega^2\tau_1^2} + \omega^2\tau_2^2 + \frac{2K_b}{3K_s}\right]^{-1/2} \quad (1)$$

where the symbols mean the following: P_0, mean power supply; C_p, sample specific heat; $f = \omega/2\pi$, chopper frequency; τ_1, sample to bath relaxation time (external); τ_2, sample + thermocouple relaxation time (internal); K_b, thermal conductance between the sample and the thermal bath; K_s, thermal conductance of the sample.

In some conditions [32], the phase shift can be reduced to

$$\alpha \approx \arcsin\left[1 + (\omega\tau_1)^{-2} + \omega^2\tau_2^2\right]^{-1/2}. \tag{2}$$

For each heating period, the frequency of the chopped light has to be low enough to avoid temperature gradients through the sample and high enough to guarantee a negligible heat dissipation from the sample to the surroundings. Under these quasi-adiabatic conditions $\alpha = 90°$ and the specific heat of the sample (C_p) is found to be [32]

$$C_p = \frac{P_0}{2\pi f \Delta T_{AC}}. \tag{3}$$

Due to the experimental difficulties in determining simultaneously ΔT_{AC} and P_0, an independent calibration of the system is required, if absolute C_p data are needed. Even in this case, the expected accuracy is not very high, which makes this technique more appropriate for relative measurements.

The adiabatic calorimeter used for the specific heat measurements together with the various experimental procedures are described in [33] and references therein. The system provides absolute specific heat values between two equilibrium states and high accurate values for the sample temperature. The C_p accuracy is 0.1% throughout the temperature range from 10 to 350 K. The absolute temperature is measured by a Pt-resistance thermometer accurately calibrated from 4.2 to 370 K. Points were obtained by two different methods: the discontinuous pulse technique and the dynamic heating thermograms. A higher accuracy is attained by the first method, whereas the second one is more appropriate for a better resolution of the C_p trace around the phase transition peaks when very low temperature rates are used.

3. Experimental results

The temperatures of the phase transitions and the shapes of the specific heat traces of C19, d-C19 and pd-C19 are in good agreement for the three different calorimetric techniques. Absolute specific heat values were obtained by DSC and adiabatic calorimetry while AC measurements were limited to relative values. In addition to the main C_p peak associated with the phase transition temperature, small anomalies of the specific heat are found at lower temperatures for the three compounds. To our knowledge this is the first time these phenomena are reported in this kind of crystals. These effects are reproducible and are observed in the various different samples used in the experiments. In the following T_i will represent the successive peak temperatures in C19 in order of decreasing temperature, starting from the temperature associated with the structural phase transition. Similarly, T_i' and T_i'' refer to the analogous sequences in d-C19 and pd-C19 respectively.

3.1. Urea/n-nonadecane

3.1.1. DSC measurements. DSC measurements on a powdered sample were performed at different heating and cooling runs around the phase transition temperature. In figure 1 we report the experimental trace from 120 to 180 K obtained from a powdered sample of C19 at 10 K min^{-1}. For this rate, the main phase transition at $T_1 = 158$ K on heating shows a thermal hysteresis of about 1 K on cooling, at least partially due to the high rate used. In addition,

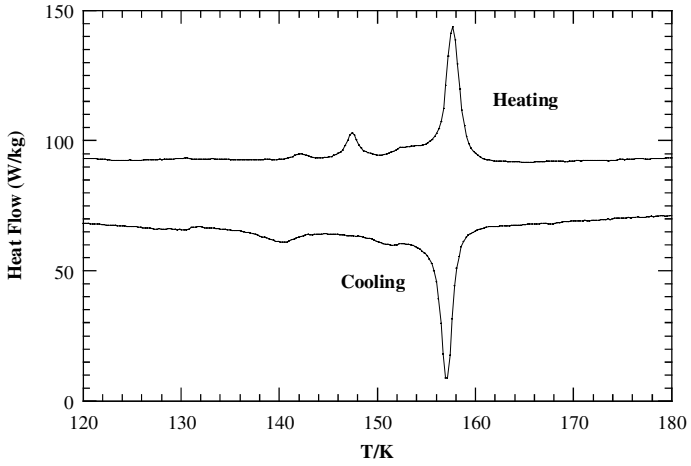

Figure 1. Differential scanning calorimetry traces for C19 at heating and cooling rates of 10 K min^{-1} on a relative scale. The peak at 158 K shows an apparent thermal hysteresis of about 1 K. Two small anomalies are also present 10 K below.

two small anomalies at $T_2 = 147$ K and $T_3 = 142$ K are found on heating. Both peaks also appear at 130 and 140 K respectively in cooling experiments when the same temperature rate is used. From these measurements the enthalpy and the entropy associated with these peaks were obtained by subtraction of a conventional straight baseline and are shown in table 2a.

3.1.2. AC measurements. A small single crystal of C19 with dimensions 2 mm × 2 mm × 0.2 mm was cut out for the AC experiments. As used in C17 for a similar sized sample [29], chopped light of 1 Hz was selected for our measurements. At room temperature, this frequency leads to a phase shift of 90° between the chopped light and the thermal response, which guarantees the validity of equation (3). The phase shift can be monitored by the lock-in amplifier used to measure the thermal oscillations ΔT_{AC}.

Figure 2 shows the AC signal obtained by the so-called quasi-isothermal method. Here, heating and cooling scans were performed in the temperature range 150–160 K with temperature increments of 0.1 K. Out of this range, the increment steps were 0.2 K. From these experiments, the main peak temperature ($T_1 = 156.54$ K, on heating) does not show any evidence of thermal hysteresis within the limits of the experimental resolution. Similar results were obtained by using a dynamic technique for various temperature rates. As an example, some data from heating and cooling experiments at a common rate of 6 K h^{-1} are plotted in figure 3. No significant differences between the dynamic and quasi-isothermal results were found. The relative C_p values (in arbitrary units) are similar in both experiments, indicating the good reproducibility of the experimental system. The shape of the specific heat peak and the value of the thermal hysteresis are the same and two small shoulders at $T_2 = 149.0$ K and $T_3 = 145.0$ K are observed (see the inset of figure 3) in agreement with the DSC measurements. It should be noted that AC experiments are performed on single crystals. The discrepancies in the temperature assignments are mainly due to the different measurement rates and the thermometry used in both techniques.

3.1.3. Adiabatic measurements. The shortcomings of the AC calorimetry for absolute results and the dynamic characteristics of DSC make it convenient to perform adiabatic measurements

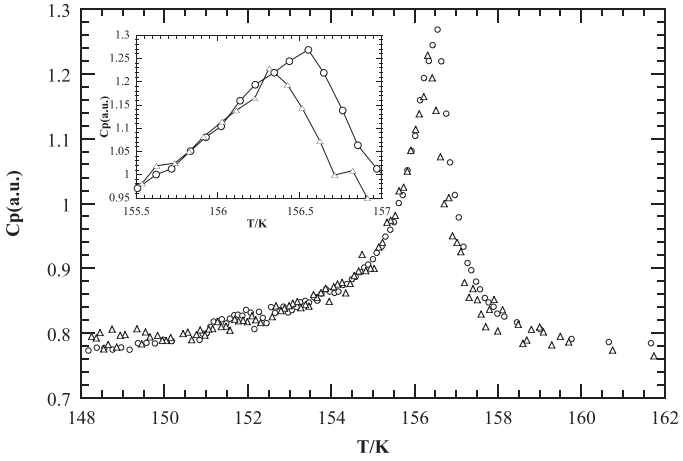

Figure 2. The AC calorimetric results for C19 around the phase transition temperature obtained by the discontinuous step technique: on heating (○) and on cooling (△). The detailed inset suggests a low thermal hysteresis of 0.1 K.

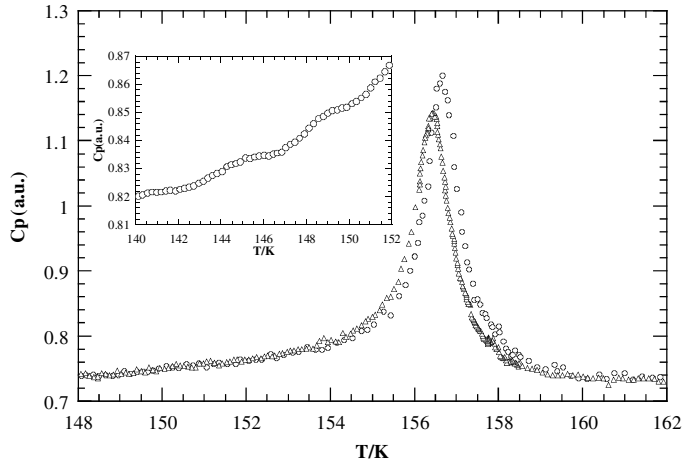

Figure 3. The specific heat of C19 by AC calorimetry: continuous heating (○) and cooling (△) at a common rate of 6 K h^{-1}. The inset shows the two small anomalies below T_1 (heating run).

to improve the accuracy of the specific heat data. In figure 4, the specific heat of a powdered sample of C19 is shown. Measurements were performed from 90 to 300 K by using the heating pulse method with temperature increments of 1 K. The maximum of the specific heat trace occurs at $T_1 = 159$ K and the shoulders observed in DSC and AC measurements are again detected at $T_2 = 147$ K and $T_3 = 143$ K. In addition, a low heating rate thermogram at 1 K h^{-1} is plotted in the same figure by means of a continuous line. This thermogram covers the temperature range from 134 to 170 K with a much better definition of the specific heat trace. Moreover, the main C_p anomaly at T_1 splits up into two different peaks not observed by AC and DSC techniques.

As done in C17 [29], detailed calorimetric studies around this temperature were performed by recording a thermogram series with heating rates varying from 100 to 0.33 K h^{-1}. Figure 5

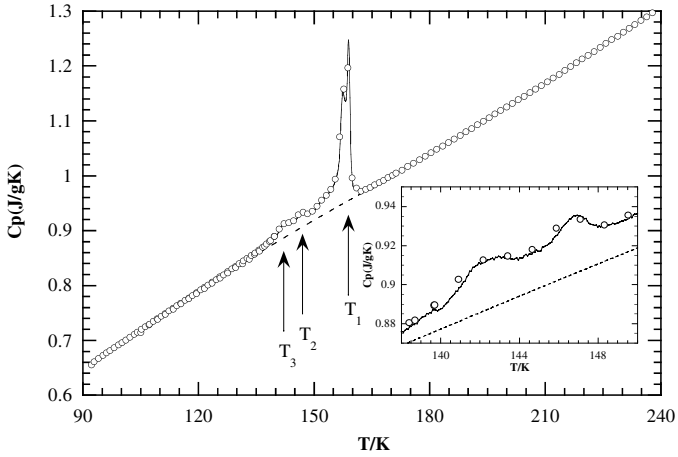

Figure 4. The specific heat of C19 obtained by adiabatic calorimetry from 90 to 240 K by using the heating pulse method (○). The temperature increments were of 1 K. The continuous line around the phase transition temperature ($T_1 = 158.77$ K) is one of the heating thermograms. Both techniques show two small anomalies at $T_2 = 147$ K and $T_3 = 143$ K. The dashed line represents the baseline used to obtain the phase transition thermodynamic functions.

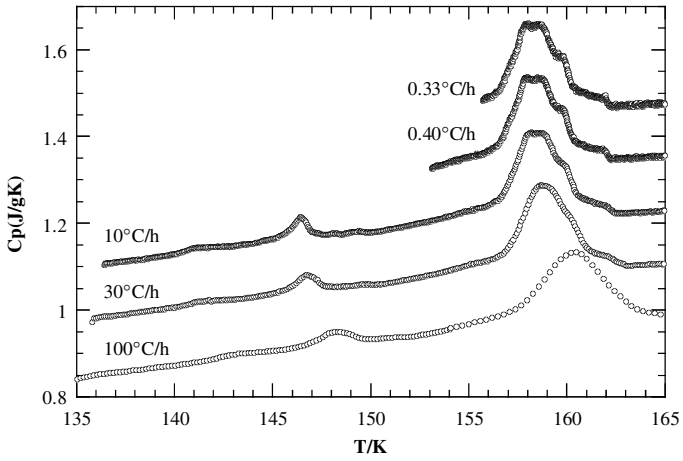

Figure 5. The C19 specific heat results obtained from five continuous heating thermograms, for various heating rates. Except for the trace at 100 K h^{-1}, the traces are shifted 0.13 J g^{-1} K^{-1} above the absolute values for the sake of clarity. The lower rates exhibit some additional anomalies around the main peak.

shows the results obtained for five selected heating rates. In order to avoid the expected influence of the thermal history effects on the phase transition, the crystal was cooled down to $T_{\min} = 120$ K after the synthesis at room temperature. The series of heating thermograms was recorded up to a maximum temperature of $T_{\max} = 170$ K. Within these conditions, results are reproducible when cycling the sample around the transition temperature, as shown for the C17 compound [29].

The low temperature peaks at T_2 and T_3 remain unchanged whereas around T_1 the main peak shows a series of secondary steps, such as found in C17. The lowest heating rate

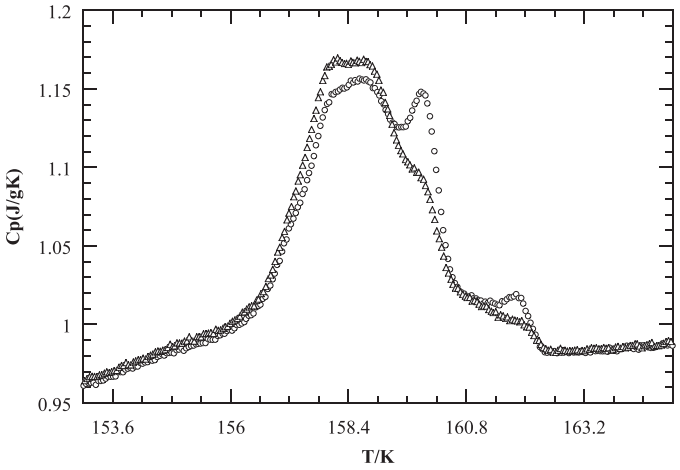

Figure 6. Two heating thermograms of C19 around the phase transition temperature at a common rate of 1 K h^{-1}. Both profiles are related to a different sample thermal history: without annealing (Δ) and after annealing (○).

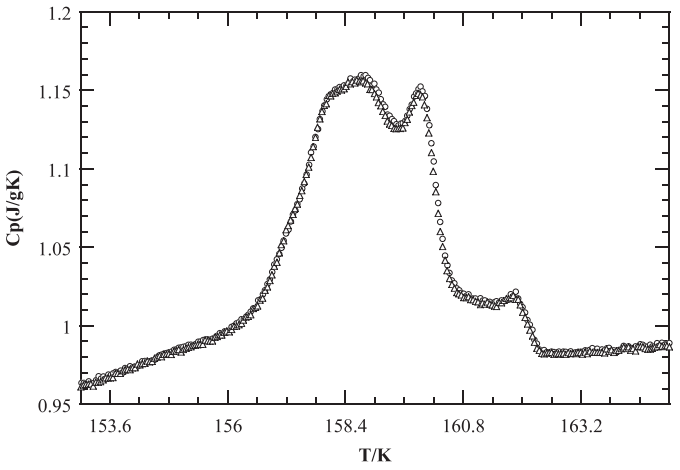

Figure 7. Reproducibility of the specific heat measurements on C19. Two independent runs at 1.0 K h^{-1} are plotted.

thermogram exhibits two small additional anomalies above T_1 and the main peak splits into two shoulders.

The main features of the C19 specific heat trace undergo remarkable changes when the sample is annealed at room temperature, as observed in the C17 compound. After this thermal treatment, the heating thermograms between T_{min} and T_{max} show a different profile, which remains unchanged if T_{max} is not surpassed in the successive cycles. The two anomalies above T_1 are steeper, and even the splitting of the main peak is more pronounced. These results are plotted in figure 6, where two heating thermograms at a common rate of 1 K h^{-1} but with different thermal histories are compared. We stress that results are always reproducible providing that heating rate and thermal history are kept unchanged. As an example, figure 7 shows two independent heating runs which illustrate this agreement.

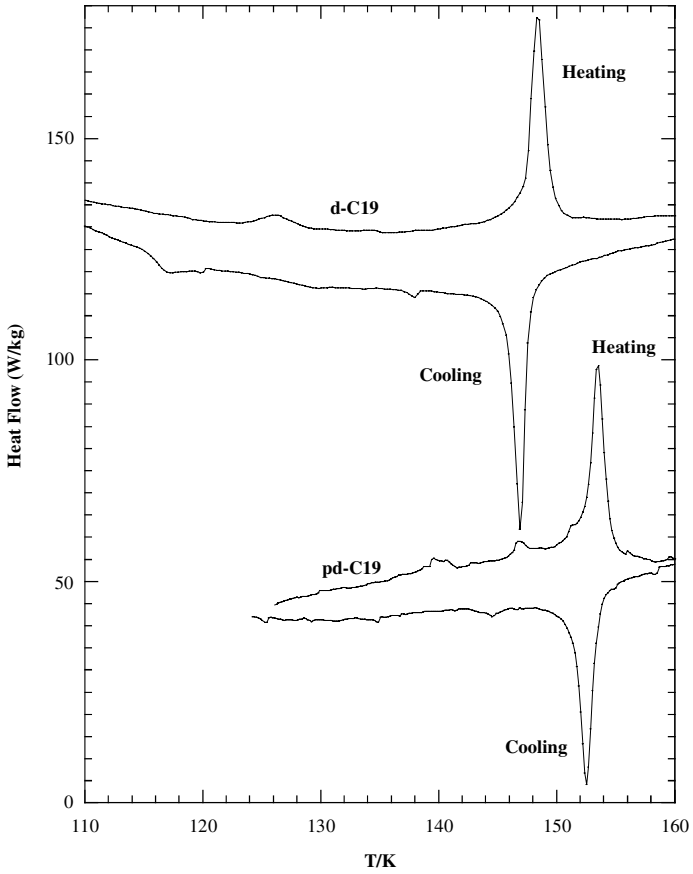

Figure 8. DSC traces for d-C19 and pd-C19 at 10 K min^{-1} heating and cooling rates in a relative scale.

3.2. Deuterated urea/n-nonadecane compounds

Our calorimetric work on this inclusion compound has been completed with the study of the specific heat of d-C19 and pd-C19. Figure 8 shows the DSC results on heating and on cooling with a temperature rate of 10 K min^{-1}. On the other hand, the adiabatic calorimetry results on d-C19 are presented in figure 9. It is observed that the phase transition temperature is lowered by total deuteration down to $T_1' = 149.4$ K, 9.4 K below T_1. In agreement with the results reported in [13], the partially deuterated compound pd-C19 undergoes the phase transition at a temperature 6 K lower than T_1, which makes the deuteration of the alkane chain primarily responsible for this effect. This is an unexpected result, because deuteration usually increases the phase transition temperature in organic compounds [34]. But up to now, this fact has not been satisfactorily explained and our macroscopic study cannot contribute to any convincing interpretation either. Below T_1', only one small C_p shoulder at $T_1' = 127.8$ K is present. This anomaly ($\Delta H \approx 0.033$ J g^{-1}) must be related to the small peaks at T_2 and T_3 of the non-deuterated compound. Furthermore, the d-C19 specific heat, which agrees with C19 below 100 K, takes progressively higher values as temperature increases. This effect is due to the deuterium higher atomic mass, which leads to lower frequency modes associated with the C–D vibrations. The contribution of these modes to the d-C19 specific heat approaches the saturated

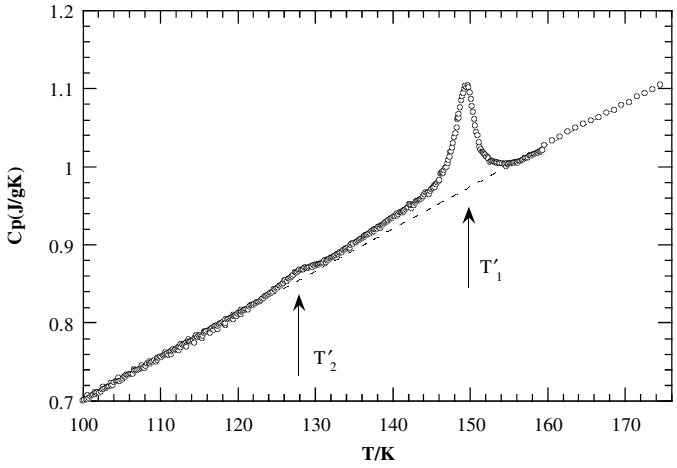

Figure 9. Specific heat trace of d-C19 (o) by adiabatic calorimetry. The dotted line represents the baseline for the calculation of the thermodynamic functions. The arrows indicate the main transition (T_1') and a small anomaly (T_2').

Table 1. Total thermodynamic functions for the phase transitions of some urea/n-alkane compounds obtained by adiabatic calorimetry. These results include the contributions of the various calorimetric anomalies present in these crystals.

	Integration temperature interval (K)	Total enthalpy (J g^{-1})	Total entropy (J g^{-1} K^{-1})
C17 [29]	130–170	1.1 ± 0.1	$(6.9 \pm 0.1) \times 10^{-3}$
C19	134–164	1.1 ± 0.1	$(7.0 \pm 0.1) \times 10^{-3}$
d-C19	125–160	0.84 ± 0.1	$(5.9 \pm 0.1) \times 10^{-3}$

values at temperatures lower than C19. As a consequence, higher C_p values above 100 K are found in d-C19.

4. Discussion

4.1. Phase transition thermodynamic functions

Using the DSC and the adiabatic data, the thermodynamic functions were obtained by means of an empirical baseline which accounts for the normal lattice contribution to the specific heat. In previous experiments on some other compounds, a careful estimation of this contribution was obtained from the vibrational spectrum and the anharmonic quantities of the solid, and was compared with the adiabatic results [35]. In the present work, the lack of experimental information limits the application of this procedure, but the small temperature range involved permits a simple extrapolation of the specific heat values at both sides of the transition temperature. A simple second order polynomial fitting accounts for the lattice contribution in C19 and d-C19 (see figures 4 and 9 respectively). After subtracting the baseline values, the usual numerical integration of C_p around a wide temperature range covering all the C_p anomalies gives the total enthalpy and entropy values. As can be seen in table 1, these results are similar in C17 within the limits of the experimental error but are slightly higher than those for d-C19.

Table 2a. Phase transitions and thermodynamic functions of C19 from various calorimetric techniques (DSC rates are 10 K min^{-1}).

	Technique						
	DSC	AC	Adiabatic	DSC	Adiabatic	DSC	Adiabatic
Peak temperature	Temperature (K)			Enthalpy (J g^{-1})		Entropy (J g^{-1} K^{-1})	
T_1 on heating	158 ± 1	156.5 ± 0.1	158.8 ± 0.1	0.59 ± 0.01	1.04 ± 0.01	$(3.7 \pm 0.1) \times 10^{-3}$	$(6.6 \pm 0.1) \times 10^{-3}$
T_1 on cooling	157 ± 1	156.3 ± 0.1	—				
T_2 on heating	147 ± 1	149.0 ± 0.1	147.0 ± 0.1	0.09 ± 0.01	0.05 ± 0.01	$(6 \pm 1) \times 10^{-4}$	$(3 \pm 1) \times 10^{-4}$
T_2 on cooling	140 ± 1	—	—				
T_3 on heating	142 ± 1	145.0 ± 0.1	143.0 ± 0.1	≈ 0.020	≈ 0.012	$\approx 1 \times 10^{-4}$	$\approx 8 \times 10^{-5}$
T_3 on cooling	130 ± 1	—	—				

Table 2b. Phase transitions and thermodynamic functions of d-C19 and pd-C19 from various calorimetric techniques (DSC rates are 10 K min^{-1}).

		Technique					
		DSC	Adiabatic	DSC	Adiabatic	DSC	Adiabatic
	Peak temperature	Temperature (K)		Enthalpy (J g^{-1})		Entropy (J g^{-1} K^{-1})	
d-C19	T_1' on heating	148.5 ± 1	149.4 ± 0.1	0.49 ± 0.01	0.81 ± 0.02	$(3.3 \pm 0.1) \times 10^{-3}$	$(5.7 \pm 0.1) \times 10^{-3}$
	T_1' on cooling	147 ± 1	—				
	T_2' on heating	126 ± 1	127.8 ± 0.1	0.07 ± 0.01	0.030 ± 0.01	$(5.5 \pm 1) \times 10^{-4}$	$(2.3 \pm 0.8) \times 10^{-4}$
	T_2' on cooling	117 ± 1	—				
pd-C19	T_1'' on heating	153.5 ± 1	—	0.40 ± 0.01	—	$(2.6 \pm 0.1) \times 10^{-3}$	—
	T_1'' on cooling	152.5 ± 1					
	T_2'' on heating	147 ± 1	—	≈ 0.015	—	$\approx 1 \times 10^{-4}$	—
	T_2'' on cooling	145 ± 1					
	T_3'' on heating	140 ± 1	—	≈ 0.030	—	$\approx 2 \times 10^{-4}$	—
	T_3'' on cooling	135 ± 1					

In tables 2a and 2b, these total values are specifically assigned to the various calorimetric anomalies present in these temperature ranges on C19 and its deuterated compounds respectively. In these tables, the DSC, AC, and adiabatic calorimetry results are also shown. The thermodynamic functions obtained from the last technique for the main phase transition in C19 and in d-C19 at T_1 and T_1' respectively are significantly higher than those obtained from DSC experiments. This is a consequence of an improved resolution and a better definition of the C_p trace determined by adiabatic calorimetry and the wider integration range used. Analogously, the enthalpic contents of the small shoulders, which are also dependent on the experimental technique, can be due to the different resolution and to the arbitrary selection of the corresponding baselines.

4.2. Order character of the phase transitions

The observed small thermal hysteresis suggest the first order character of the phase transition in C19 as in the case of C17 [29], but the thermal hysteresis is near the temperature resolution of the AC results. In the case of DSC measurements a shift of the peak temperature on heating and cooling experiments is always found as a consequence of the high temperature rates usually

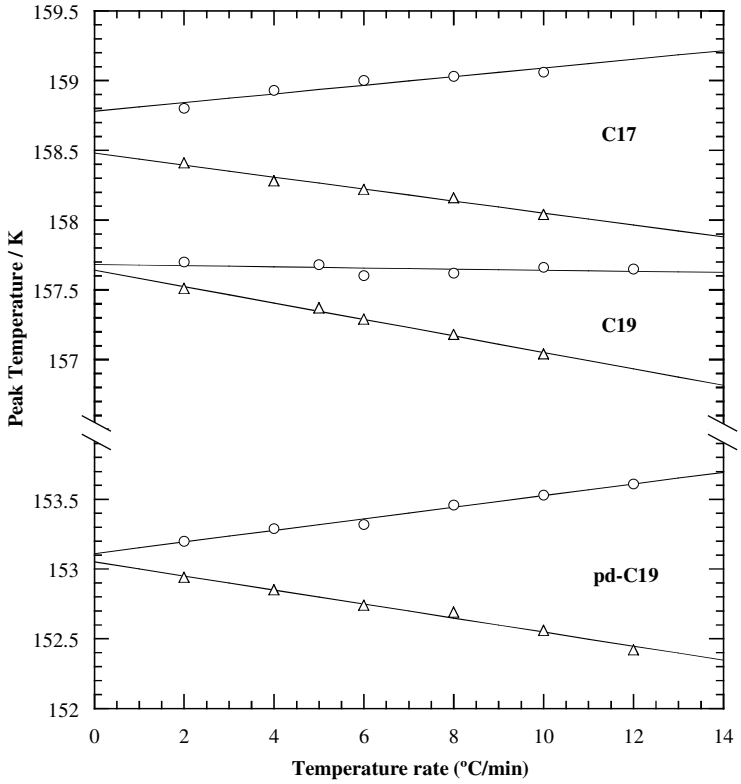

Figure 10. Peak temperature versus temperature rate in C17, C19, and pd-C19 from DSC measurements. O, heating runs; Δ, cooling runs. Linear extrapolations to zero rate limit the thermal hysteresis for C19 and pd-C19 to 0.04 and 0.06 K respectively, whereas the value for C17 is 0.30 K.

involved. However, measurements under various heating and cooling rates permit a reliable estimation of the intrinsic thermal hysteresis by extrapolation of the observed peak temperatures to zero rates. In figure 10 the measured peak temperatures of these compounds for rates varying from 2 to 12 K min^{-1} are presented. The extrapolated value limits the possible sample thermal hysteresis down to only 0.04 K. A similar study for the partially deuterated compound pd-C19 shows the phase transition temperature at about 153 K and also a very low thermal hysteresis of 0.06 K, as can be seen in figure 10. However, this last quantity rises up to 0.30 K in C17 in agreement with the adiabatic data (0.25 K), and again confirms the first order character of this phase transition [29].

We can also look for evidence of the possible latent heat associated with the phase transition. Though latent heat cannot be measured by the AC technique, its presence can be inferred as it affects the shape of the calorimetric signal obtained by different experimental conditions. In the quasi-static method, the latent heat is only provided by the sample surroundings (mainly by the thermal block) and it is not measured at all. This means that in pure first order phase transitions, where only latent heat is present in the transition, no peak should be observed. However, in dynamic procedures, the pulse heat is also absorbed or released at the transition temperature, which damps the sample thermal oscillations ΔT_{AC}, and by equation (3) leads to apparent higher values of C_p. This contradictory behaviour is

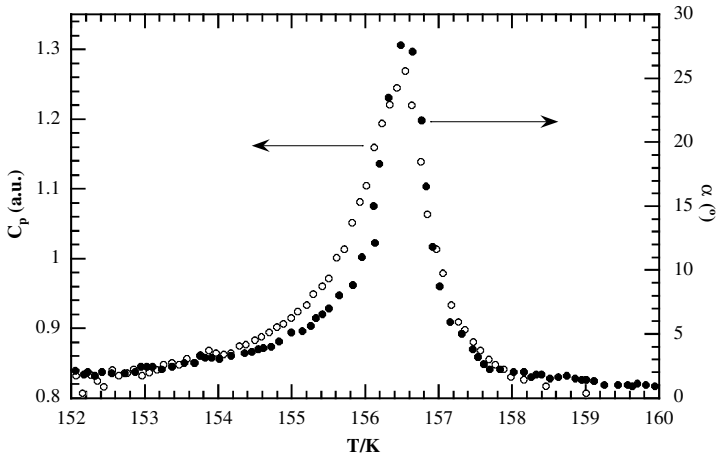

Figure 11. The phase shift, α, around the C19 phase transition range (•) and the specific heat (○) are compared. A similar peak for both quantities is found.

found in well defined first order phase transitions such as in martensitic transformations [36]. However, the AC results do not show any noticeable difference between the two measurement procedures and do not support any conclusive decision about the order character of the C19 phase transition. A similar behaviour was observed in the AC measurements of C17 but, as cited above, the first order character has been firmly established for this compound. We can conclude that the latent heat associated with these phase transitions, if present, is very small.

As cited in previous works [37, 38], the phase shift α between the sample thermal oscillations and the incident heating pulses is often considered as a positive test for the order character of the phase transition. In particular, the phase shift tends to show an abrupt variation in first order phase transitions and smoother changes in second order phase transitions. In our case, the high increase of the phase shift at the transition temperature would suggest a first order character of this transformation (figure 11).

However, from equation (2) and accepting $\omega\tau_2 \to 0$, we obtain

$$\tan\alpha = \omega\tau_1 = \omega C_p/K_b \tag{4}$$

K_b, which accounts for the thermal link between the sample and the surroundings, is not significantly dependent on the temperature in the vicinity of T_1 and a linear relation between the phase and the sample specific heat takes place. Consequently, the claimed phase-testing to discriminate the order of the phase transition is only a direct effect of the specific heat behaviour around it. Abrupt peaks and smooth anomalies are usually related to first and second order phase transitions respectively, but this has never been a reliable test for such definitive conclusions. Moreover, the validity of equation (4) affects the requirements for equation (3) to be valid around the phase transition temperatures, where the specific heat values are not constant. This fact is independent of the phase transition character, though it should be more relevant in first order phase transitions. As a consequence, the rejected terms in equation (1) should be considered in all these cases, if absolute values of C_p are required.

On the other hand, the first order character of the possible phase transitions associated with the couple of C_p small anomalies for C19 and pd-C19 and the single one for d-C19 would be beyond doubt due to the high thermal hysteresis found in all these cases. The physical mechanisms driving these last subtle effects remain unknown.

4.3. Thermal history

As regards the thermal history exhibited by C19 and C17, recent NMR and x-ray diffuse scattering experiments and Monte Carlo calculations [13] have shown some pre-transitional short range effects which appear when approaching the phase transition on cooling. These effects seem to start at temperatures far above the transition temperature and are related to the presence of clusters in which the alkane chains present the orientational order characteristic of the low symmetry phase. In this situation, the pre-transitional fluctuations of the alkane chains make the hexagonal symmetry of the crystal an averaged result. This description could explain the different profile of the calorimetric traces in C17 and C19 when cycling near the phase transition than when the sample is heated to room temperature, far above the range where the pretransitional effects take place.

4.4. Specific heat contributions

As cited above, the accuracy of the phase transition thermodynamic functions could be improved if, as done in some other crystals [39], precise baselines for the normal lattice contribution to the specific heat were calculated from the vibrational spectrum data. Even a partial knowledge of the density of state function has permitted a good fit to the experimental specific heat around room temperature in some cases. Moreover, the anharmonic quantities such as the Gruneisen parameter and the isothermal compressibility, which are difficult to measure by other techniques, can be determined [40]. At present, the required spectroscopic information for this purpose is not available in urea/n-alkanes. As a first approach, a provisional analysis of the various contributions to the specific heat can be explored. Leaving apart the anomalies associated with the phase transitions, both C17 and C19 present very similar values of C_p. This is the result of two main contributions: one due to the urea lattice and the other to the alkane guest, provided that coupling of both sublattices which interact by means of weak Van der Waals forces be neglected. High frequency modes associated with the internal bonds in both the urea and alkane sublattices which are responsible for the specific heat trace shape at high temperatures ($\approx$ above 120 K) are not expected to undergo significant changes under different crystal environments. This effect is clearly observed in related crystals where alkane chains are included in a different structure, such as in $(C_nH_{2n+1}{\cdot}NH_3)_2MCl_4$ layer compounds [41]. The specific heat of these solids is characterized by an inflexion point in the C_p trace at about 160 K, which can be assigned to the presence of these two independent sets of normal modes as well as to the emerging anharmonic effects around this temperature. This fact suggests a tentative approach for a deconvolution of C17 and C19 specific heat. Primary empirical calculations by using the available data of the pure urea specific heat [42, 43] permit us to estimate the contribution of the alkyl chain. This approach is shown in figure 12, where the dashed line represents the urea specific heat per gram of C19, whereas the square dots stand for the corresponding estimated alkyl contribution. In figure 13 we compare this last result with the CH_2 contribution in the alkyl chain of $(C_nH_{2n+1}{\cdot}NH_3)_2MCl_4$ layer compounds (continuous line) [41]. One should notice the similar shape shown by both traces and the expected inflexion point at 170 K, all of which indicates that this first rough approach leads to somewhat reasonable results. For C19 the specific heat tentatively assigned to the alkyl chain only reaches 90% of the value for layer compounds. This discrepancy should be assigned to the influence of the different crystal environment. In both cases, the crystal stability is guaranteed by the hydrocarbon chains, which is a clear indication of the interaction between the two sublattices, but in C19 the urea tunnels specifically hinder the alkane transverse displacements, whereas in layer compounds the alkyl chains are less constrained to move.

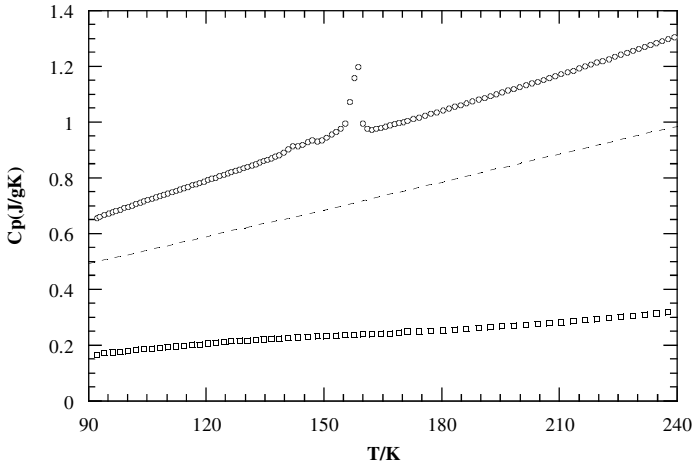

Figure 12. Some of the C19 specific heat points obtained by adiabatic calorimetry (○). The dashed line represents the urea specific heat per gram of C19 and (□) the corresponding alkyl contribution.

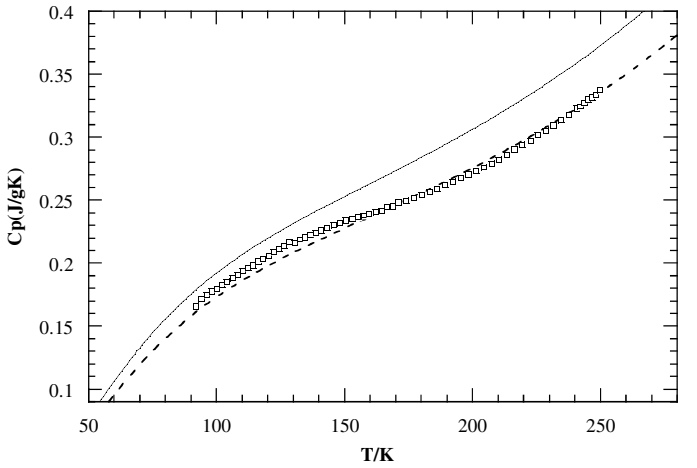

Figure 13. The alkyl chain contribution in C19 (□) compared with some other layer compounds (continuous line). They show a 10% discrepancy due to the different crystal environment. The dotted line is 90% of this last contribution.

4.5. Final remarks

In summary, C17 and C19 show a very similar experimental behaviour as expected for a quasi-identical host crystal structure, the different length of the alkane chains being the only remarkable point. It is worth noting that the observed behaviour of the specific heat of the free n-alkanes attains an asymptotic common value for $n \rightarrow \infty$ [44], with negligible differences for $n > 10$. This fact, together with the relative uncoupling of urea and n-alkane substructures, could explain the good agreement between C17 and C19 specific heats as well as their phase transition thermodynamic function values. It seems that a simplified model of infinite length urea tunnels filled with a continuous hydrocarbon chain could explain the main features of the physical properties of these compounds. In both cases, the calorimetric

response is influenced by the thermal history and by the measurement temperature rates. The former effect could be partially assigned to the presence of pretransitional effects above the transition temperature [13]. Moreover, the results obtained for C17 suggest that the dynamical processes of the orientational disorder in the high temperature phase at room temperature are also responsible for this behaviour. A brief discussion of these mechanisms and the required relaxation times for thermodynamic equilibrium are discussed in [29]. The experimental information about urea/n-alkane compounds agrees with a progressive ordering of the alkane molecules around the phase transition temperature. Our calorimetric data are consistent with this interpretation, if the guest ordering process takes place in successive steps and spreads over a wide temperature interval. In the case of C19 this range is extended from 130 to 160 K. Leaving apart the confirmed reproducibility of these results, both in powdered and in single crystal samples, it is not clear whether the stepped ordering is a consequence of the very small heating rates involved or, on the contrary, higher rates mask this behaviour.

However, the experimental behaviour of these compounds presents some small but clear differences. This fact shows the failure of oversimplified models and can only be related to the length of the alkane chains. This influence is achieved in different ways: first, the alkane accommodation in the urea tunnels controls the gap between adjacent molecules and consequently the incommensurability ratio values. Second, the number of CH_3 end-groups and their related interactions are different. Finally, as found in most compounds with alkyl chains, 'even' and 'odd' compounds behave differently. For example, the phase transition temperature is found to depend on the alkane chain length for 'odd' compounds [20] though this effect is negligible for C15 [21], C17 and C19, which undergo their phase transition at nearly the same temperature. Moreover, the small anomalies present in C19 are not observed in C17. Contrarily to the first order character of the C17 phase transition, the results obtained in C19 are not conclusive. The apparent thermal hysteresis observed in C19 lies in the limits of the experimental resolution and no phase boundaries are found in optical experiments. Single crystal deuterium NMR results together with a simplified model for the reorientational jumps of the guest molecules lead to similar inconclusive results and do not permit any further conclusion about the complex physical mechanisms present in these phase transitions. As a consequence, more detailed experimental investigations are needed. At present optical and elastic measurements are in progress and together with the calorimetric results will be the basis of a phenomenological description of these phase transitions [45]. Preliminary results show the inadequacy of simplified models which only takes into account the structural transformation undergone by the urea sublattice. This is again a clear indication of the influence of the alkane chain orientational ordering in the mechanism of these phase transitions.

Acknowledgments

The authors acknowledge financial support from the University of the Basque Country (project No UPV 13646/2004) and the Ministry of Science and Technology (project No MAT2004-03166), as well as from the Basque Government in the frame of the Strategic Plan for Science and Technology (ETORTEK-ACTIMAT-2005).

References

[1] Takemoto K and Sonoda N 1984 *Inclusion Compounds* (London: Academic)
[2] Smith A E 1952 *Acta Crystallogr.* **5** 224
[3] George A R and Harris K D M 1995 *J. Mol. Graphics* **13** 138
[4] Harris K D M and Thomas J M 1990 *J. Chem. Soc. Faraday Trans.* **86** 2985

[5] Weber T, Boysen H and Frey F 2000 *Acta Crystallogr.* B **56** 132
[6] Casal H L 1990 *J. Phys. Chem.* **94** 2232
[7] Kobayachi M, Koizumi H and Cho Y 1990 *J. Chem. Phys.* **93** 4659
[8] El Baghdadi A and Guillaume F 1995 *J. Raman Spectrosc.* **26** 155
[9] Casal H L, Cameron D G and Kelusky E C 1984 *J. Chem. Phys.* **80** 1407
[10] Grenfield M S, Vold R L and Vold R R 1985 *J. Chem. Phys.* **83** 1440
[11] El Baghdadi A, Dufourct E F and Guillaume F 1996 *J. Phys. Chem.* **100** 1746
[12] Schmider J and Müller K 1998 *J. Phys. Chem.* A **102** 1181
[13] Le Lann H, Odin C, Toudic B, Ameline J C, Gallier J, Guillaume F and Breczewski T 2000 *Phys. Rev.* B **62** 5442
[14] Cannarozzi G M, Meresi G H, Vold R L and Vold R R 1991 *J. Phys. Chem.* **95** 1525
[15] Guillaume F, Sourisseau C and Dianoux A J 1990 *J. Chem. Phys.* **93** 3536
[16] Guillaume F, Sourisseau C and Dianoux A J 1991 *J. Chem. Phys.* **88** 1721
[17] Bourgeois L, Ecolivet C, Toudic B, Bourges P and Breczewski T 2003 *Phys. Rev. Lett.* **91** 255041
[18] Schmider J, Van Smaalen S, De Boer J L, Haas C and Harris K D M 1995 *Phys. Rev. Lett.* **74** 734
[19] Ollivier J, Ecolivet C, Beaufils S, Guillaume F and Breczewski T 1998 *Europhys. Lett.* **43** 546
[20] Pemberton R C and Parsonage N G 1965 *Trans. Faraday Soc.* a **61** 2112
[21] Pemberton R C and Parsonage N G 1966 *Trans. Faraday Soc.* a **62** 553
[22] Etrillard J, Lasjaunias J C, Toudic B, Guillaume F and Breczewski T 2000 *Europhys. Lett.* **49** 610
[23] Vold R L, Vold R R and Heaton N J 1989 *Adv. Magn. Reson.* **13** 17
[24] Lee K J, Mattice W L and Snyder R G 1992 *J. Chem. Phys.* **96** 9138
[25] Souaille M, Guillaume F and Smith J C 1996 *J. Chem. Phys.* **105** 1516
[26] Lefort R, Toudic B, Etrillard J, Guillaume F, Bourges P, Currat R and Breczenski T 2001 *Eur. Phys. J.* B **24** 51
[27] Rabiller P, Etrillard J, Toupet L, Kiat J M, Launois P, Petricek V and Breczenski T 2001 *J. Phys.: Condens. Matter* **13** 1653
[28] Lynden-Bell R M 1993 *Mol. Phys.* **79** 313
[29] Fraile-Rodriquez A, Ruiz-Larrea I, Rubio-Peña L and López-Echarri A 2001 *Eur. Phys. J.* B **24** 189
[30] Rubio-Peña L, Breczewski T and Bocanegra E H 2002 *Ferroelectrics* **269** 171
[31] Fraile-Rodríguez A, Ruiz-Larrea I and López-Echarri A 2001 *Thermochim. Acta* **377** 131
[32] Sullivan P F and Seidel G 1968 *Phys. Rev.* **173** 679
[33] Igartua J M, Ruiz-Larrea I, Zubillaga J, López-Echarri A and Couzi M 1992 *Thermochim. Acta* **199** 35
[34] Asaji T, Yoza M and Ishizaka T 1999 *J. Phys.: Condens. Matter* **11** 5219
[35] Ruiz-Larrea I, Fraile-Rodríguez A, Arnaiz A and López-Echarri A 2000 *J. Therm. Anal. Calorimetry* **61** 503
[36] Fraile-Rodríguez A, Ruiz-Larrea I, López-Echarri A and San Juan J 2006 *Scr. Mater.* **54** 1199–203
[37] Garland W 1985 *Thermochim. Acta* **88** 127
[38] Castro M 1995 *PhD Thesis* C.S.I.C. Universidad de Zaragoza, Spain
[39] López-Echarri A, Zubillaga J and Tello M J 1988 *Solid State Commun.* **68** 185
[40] López-Echarri A, Ruiz-Larrea I, Díaz-Hernandez J, Aguirre-Zamalloa G and Tello M J 1997 *Phase Transit.* **64** 1
[41] López-Echarri A, Zubillaga J and Tello M J 1988 *Solid State Commun.* **68** 185
[42] Ruehrwein R A and Huffman H M 1946 *J. Am. Chem. Soc.* **68** 1759
[43] Kozyro A A, Dalidovich S V and Krasulin A P 1986 *J. Appl. Chem. USSR* **59** 1353
[44] Huang D, Simon S L and McKenna G B 2005 *J. Chem. Phys.* **122** 849071
[45] Breczewski T *et al* 2007 *J. Phys. Chem.* B to be published